NSF regulates membrane traffic along multiple pathways in Paramecium.

Roland Kissmehl, Marine Froissard, Helmut Plattner, Massoud Momayezi, Jean Cohen

NSF regulates membrane traffic along multiple pathways in *Paramecium*

Roland Kissmehl[1],[*],[‡], Marine Froissard[2],[*], Helmut Plattner[1], Massoud Momayezi[1] and Jean Cohen[2]

[1]University of Konstanz, Department of Biology, PO Box 5560, 78457 Konstanz, Germany
[2]Centre de Génétique Moléculaire, CNRS, Avenue de la Terrasse, 91198 Gif-sur-Yvette Cedex, France
*These authors contributed equally to this work
‡Author for correspondence (e-mail: roland.kissmehl@uni-konstanz.de)

Summary

N-ethylmaleimide (NEM)-sensitive factor (NSF), a regulator of soluble NSF attachment protein receptors (SNAREs), is required for vesicular transport in many eukaryotic cells. In the ciliated protozoon *Paramecium,* complex but well-defined transport routes exist, constitutive and regulated exocytosis, endocytosis, phagocytosis and a fluid excretory pathway through contractile vacuoles, that can all be studied independently at the whole cell level. To unravel the role of NSF and of the SNARE machinery in this complex traffic, we looked for NSF genes in *Paramecium*, starting from a partial sequence found in a pilot random sequencing project. We found two very similar genes, *PtNSF1* and *PtNSF2*, which both seem to be expressed. Peptide-specific antibodies (Abs) recognize PtNSF as a 84 kDa band. *PtNSF* gene silencing results in decreasing phagocytotic activity, while stimulated exocytosis of dense core-vesicles (trichocysts), once firmly attached at the cell membrane, persists. Ultrastructural analysis of silenced cells shows deformation or disappearance of structures involved in membrane traffic. Aggregates of numerous small, smooth vesicles intermingled with branches of ER occur in the cytoplasm and are most intensely labeled with anti-NSF Ab-gold. Furthermore, elongated vesicles of ~30 nm diameter can be seen attached at cortical calcium storage compartments, the alveolar sacs, whose unknown biogenesis may thus be revealed. Involvement of PtNSF in some low frequency fusion events was visualized in non-silenced cells by immuno-fluorescence, after cautious permeabilization in the presence of ATP-γ-S and NEM. Our data document that PtNSF is involved in distinct pathways of vesicle traffic in *Paramecium* and that actual sensitivity to silencing is widely different, apparently dependent on the turnover of membrane-to-membrane attachment formation.

Key words: Ciliates, *Paramecium*, Secretion, Phagocytosis, Golgi, Endoplasmic reticulum

Introduction

In eukaryotes, membrane traffic is mediated by vesicle budding from donor compartments and targeted fusion with specific acceptor organelles, where they deliver their cargo (Rothman and Wieland, 1996). In the past decade enormous efforts have been made to elucidate the molecular components involved in the regulation of these steps. Complementary approaches (e.g., biochemistry, in vitro studies and genetics in yeast) led to the discovery of essential protein partners (Augustine et al., 1999; Jahn and Südhof, 1999). One of them, NSF (N-ethylmaleimide sensitive factor), is a homohexameric ATPase that functions together with SNAPs (soluble NSF attachment proteins) and SNAREs (SNAP receptors) in vesicular transport of many cells (Owen and Schiavo, 1999; May et al., 2001; Whiteheart et al., 2001). NSF is thought to act as a molecular chaperone (Morgan and Burgoyne, 1995) controlling the conformation of vesicle (v)- and target (t)-SNAREs, which must be complexed in trans configuration between both membranes before fusion can occur (Söllner et al., 1993a; Söllner et al., 1993b; Hanson et al., 1997).

A NSF protomer contains three distinct domains (May et al., 2001; Whiteheart et al., 2001): an N-terminal domain (N) responsible for interaction with the α-SNAP-SNARE complex and two homologous ATP-binding domains (D1 and D2). The ability of the D1 domain to hydrolyze ATP is required for NSF activity, while the D2 domain is required for hexamerization. The sequences of NSF-D1 and NSF-D2 place NSF in the AAA (ATPases associated with various cellular activities) superfamily (Neuwald et al., 1999). Such proteins contain at least one copy of a conserved, ~230 amino acid cassette with a characteristic phosphate-binding P-loop (Walker A) and a metal ion-binding DEXX box (Walker B) nucleotide-binding sequence.

In a *Paramecium* cell, several clearly defined vesicle transport routes exist (Allen, 1988; Plattner, 1993). The import routes include coated vesicle-mediated endocytosis and non-coated phagocytosis (Allen and Fok, 2000). Several export routes exist, including constitutive and stimulated exocytosis of dense core-vesicles (trichocysts) (Plattner et al., 1991; Plattner, 1993; Vayssié et al., 2000), defecation of spent phagosomes at the cytoproct (Allen and Fok, 2000), and fluid release by the osmoregulatory contractile vacuole (Allen, 2000). Internal fusion processes involve the route endoplasmic reticulum (ER) → Golgi apparatus [e.g. for the biogenesis of constitutive secretory vesicles (Flötenmeyer et al., 1999) and the biogenesis of trichocysts (Momayezi et al., 1993; Gautier

et al., 1994)], delivery from endocytotic vesicles via early endosomes to the compartments of the digestive cycle (Allen et al., 1992; Flötenmeyer et al., 1999), membrane recycling from the cytoproct to the nascent food vacuole (Allen et al., 1995), fusion and retrieval of different vesicle types along the digestive cycle, as well as any membrane recycling along the precisely coordinated intracellular digestive cycle (Allen and Fok, 2000).

In the present study, starting from the recent identification of a NSF partial sequence in a pilot genome project (Dessen et al., 2001; Sperling et al., 2002), we cloned two *PtNSF* genes from *Paramecium tetraurelia*. Gene silencing, light and electron microscope (EM) and immunolocalization analyses reveal a ubiquitous involvement of PtNSF in vesicle traffic occurring in *Paramecium*, which thus shows its advantages for studies of NSF functions.

Materials and Methods

Cell culture and test of exocytosis capacity
Wild-type strains of *Paramecium tetraurelia* used were stock 7S or d4-2, derived from stock 51 (Sonneborn, 1974). Cells were grown in grass infusion (Wheat Grass Powder, Pines International, Lawrence, KS), bacterized with *Klebsiella pneumoniae* the day before use, and supplemented with 0.4 $\mu g \cdot ml^{-1}$ β-sitosterol (Sonneborn, 1970), or, for subcellular fractionation, in axenic medium (Kaneshiro et al., 1979). Trichocyst exocytosis capacity was visualized by a saturated solution of picric acid (Vayssié et al., 2000).

Cell fractionation
Cell surface complexes (isolated 'cortices') were prepared as described (Vilmart-Seuwen et al., 1986). Other cell fractions were prepared from sterile cell cultures as previously described (Kissmehl et al., 1998). Protein concentrations were determined with BSA as a standard (Bradford, 1976).

PCR of genomic DNA
Total wild-type DNA for PCR was prepared from log-phase cultures as described (Duharcourt et al., 1995). The short probe consisted of a 336 bp PCR amplification product with *PtNSF1* specific primers:
    oligonucleotide 1: 5′-GAACTCAAGGTGAAAAGAAG-3′
    oligonucleotide 2: 5′-TTGATTGATTATGGCTCCTTCAG-3′.
Each PCR reaction (50 μl) contained 150 ng of DNA, 50 pmol of each primer, 0.2 mM of each dNTP and 2.5 U of Taq DNA polymerase (Roche Diagnostics). Reactions were carried out for one cycle of denaturation (1 minute, 92°C), and 30 cycles of denaturation (30 seconds, 92°C), annealing (45 seconds, 54°C) and extension (90 seconds, 72°C), with a final extension step (10 minutes, 72°C).

The long probe, consists of a 2310 bp amplification product with *PtNSF1* specific primers:
    oligonucleotide 3: 5′-TCTAACTATTACCAGTTGCTC-3′
    oligonucleotide 4: 5′-GGTGATTCATAATCACTGTAG-3′.
The product was obtained with the kit Expand Long Template PCR System (Roche Diagnostics). Each reaction (50 μl), adjusted to a concentration of nucleotides corresponding to the *Paramecium* A+T rich genome composition (740 nM of dATP and dTTP; 260 nM of dCTP and dGTP), contained 150 ng of DNA, 50 pmol of each primer and 3 U of polymerase mix. Amplification was performed with one cycle of denaturation (92°C, 2 minutes), 10 cycles of denaturation (92°C, 10 seconds), annealing (55°C, 30 seconds), extension (68°C, 210 seconds), then 20 cycles of denaturation (92°C, 10 seconds), annealing (55°C, 30 seconds), extension (68°C, 210 seconds plus 15 seconds/cycle) with a final extension step (68°C, 7 minutes).

PCR of cDNAs
The open reading frames (ORFs) of *PtNSF1* and *PtNSF2* were amplified from a *P. tetraurelia* 51S cDNA library (Klumpp et al., 1994) in λZAP Express (Stratagene GmbH, Heidelberg, Germany) using polymerase chain reaction (PCR) performed with the Advantage 2 PCR Kit (Clontech, Heidelberg, Germany). The reaction (50 μl) contained 200 μM each of the four nucleotides (dATP, dTTP, dCTP, dGTP), 3 μl of the cDNA library (3×10^5 plaque-forming units), 20 pmol of each primer and 1 μl of Advantage 2 polymerase mix. In the case of *PtNSF1* the primers used were:
    oligonucleotide 5: 5′-TTCAGCAAAAGCATTCTAAC-3′
    oligonucleotide 6: 5′-AAATAAATTAATCTCAAAGGTG-3′,
both containing artificial restriction sites added at their 5′-ends (*Spe*I and *Bam*HI, respectively). The same is true for oligonucleotides 7 and 8, which are specific for *PtNSF2*:
    oligonucleotide 7: 5′-ATGATTCCAGCAAAGGCATTCTAACTA-CTACCAG-3′
    oligonucleotide 8: 5′-CTACTAATAATAAATAATCCTCAAAG-3′.
Amplification of *PtNSF1* was performed with one cycle of denaturation (95°C, 1 minute), 35 cycles of denaturation (95°C, 30 seconds), annealing (54°C, 45 seconds) and extension (68°C, 3 minutes), followed by a final extension step at 68°C for 3 minutes. In the case of *PtNSF2*, the annealing temperature was 62°C and the number of cycles was increased to 55.

PtNSF1-specific products were purified using the QIAquick PCR Purification Kit (Qiagen) and digested by *Spe*I and *Bam*HI (10 units each, 2 hours, 37°C). Double-digested cDNA was then extracted from low-melt TAE agarose gels using the QIAquick gel extraction kit (Qiagen) and ligated into the plasmid pBluescript II SK⁻ (Stratagene GmbH), digested with the same enzymes. *PtNSF2*-specific PCR products were cloned into the plasmid pTAdv by using the AdvanTAge™ Cloning Kit (Clontech) according to the manufacturer's instructions. After transformation into *E. coli* (DH5α cells or TOP10F′ cells), positive clones were sequenced as described below.

Homology-dependent gene silencing
For silencing experiments, PCR products amplified in the same conditions as for the long probe were purified by QIAquick PCR Purification Kit (Qiagen, Hilden, Germany), filtered on Millex-GV (0.22 μm) (Millipore, Bedford, MA), precipitated and resuspended in water at a final concentration between 10 and 30 μg/μl. Before microinjection, wild-type cells were treated with a solution of aminoethyldextran (Plattner et al., 1984) at 0.01% to stimulate trichocyst exocytosis before microinjection, thus avoiding any further discharge that could disturb microinjection. This does not interfere with the analysis of exocytosis since a full complement of trichocysts is resynthesized within less than 7 hours (Plattner et al., 1993), whereas the first signs of silencing appear after at least 16 hours at 27°C. DNA microinjections were made under an inverted Nikon phase-contrast microscope, using a Narishige micromanipulation device, and an Eppendorf air-pressure microinjector as described (Ruiz et al., 1998; Galvani and Sperling, 2001).

The *PtNSF* silencing effect on cells clonally derived from microinjected cells can be recognised after 24 hours and 48 hours of growth at 27°C by reduced phagocytic activity before cell lethality occurs (see Results). Therefore, the efficiency of silencing was tested by adding India ink to the medium to follow food vacuole formation over a 10 minute period. NSF-silenced cells do not form any food vacuoles, whereas ~10 are formed in normal cells over a 10 minute period.

Preparation of radioactive probes
Probes were synthesised by [α-³²P]dATP incorporation using a Random Primers Labeling System (Gibco-BRL, Cergy-Pontoise, France), according to the supplier's protocol.

Southern blots

Paramecium DNA was digested by restriction enzymes according to the manufacturer's instructions (New England Biolabs, Beverly, MA), then fractionated by electrophoresis on 1% agarose gels and transferred to Hybond-N+ filters. Hybridizations were carried out as described (Church and Gilbert, 1984), at 60°C. The membranes were then washed at the same temperature with decreasing concentrations of SSC, in the presence of 0.1% SDS as follows: 2× SSC for 30 minutes and 0.2× SSC for 30-45 minutes (Sambrook et al., 1989). Images were obtained by using a Phosphorimager (Molecular Dynamics, Sunnyvale, CA). Hybridizations were quantified by ImageQuant Software (Molecular Dynamics).

RNA extractions and northern blots

Total RNA was prepared essentially as described (Chomczynski and Sacchi, 1987) by using the Trizol reagent (Gibco BRL), except that the cells were lysed by vortexing in the presence of glass beads. Total RNA was fractionated on formaldehyde/1.25% agarose gels, and transferred to positively charged nylon membranes (Ambion, Austin, TX) by capillarity. Hybridization was carried out at 50°C in 6× SSC, 2× Denhardt's solution and 0.1% SDS (Sambrook et al., 1989); the filters were then washed and imaged as described for a Southern blot.

Sequencing

The sequencing was either made on an AbI 310 sequencer using the BigDye Primer Cycle Sequencing Ready Reaction Kit (Perkin Elmer, Foster City, CA) or made by MWG Biotech custom sequencing service. Overview sequencing of different library clones hybridizing with a *PtNSF1* probe was made with a single primer:

oligonucleotide 9: 5′-GAAGGAGCCATAATCAATC-3′.

DNA sequences were aligned either by the CLUSTAL W or by the JOTUN HEIN method, both integrated in the DNASTAR Lasergene software package (Madison, WI).

Peptide synthesis and antibody preparation

Synthesis and immunisation of a peptide corresponding to the amino acid sequence of *Paramecium* PtNSF1 (NH_2-CF$_{464}$QKKLNKQDEL-KVKRSDF$_{481}$-CONH$_2$) was carried out by Pineda (Antikörper-Service, Berlin, Germany). The peptide also contains an additional cysteine at the N-terminus. For immunisation the peptide was coupled to keyhole-limpet haemocyanin and injected into rabbits and guinea pigs as previously described (Hauser et al., 1998). Antibodies (Abs) were affinity-purified using the same peptide immobilised on CNBr-activated Sepharose 4B (~3 ml, at about 3 mg/ml).

SDS-PAGE and immunoblotting

Protein samples were denatured by boiling for 3 minutes in SDS sample buffer, subjected to electrophoresis either on 10% SDS polyacrylamide gels using a discontinuous buffer system described previously (Laemmli, 1970). The replicas were electroblotted to nitrocellulose membranes and immuno reactions were carried out as described (Kissmehl et al., 1997) by using affinity-purified Abs against yeast NSF, Sec18p (Mayer et al., 1996), or against a peptide of *Paramecium* PtNSF1 (see above). Bound Abs were detected with the corresponding peroxidase-conjugated secondary Ab (anti-rabbit IgG or anti-guinea pig IgG) using the Amersham enhanced chemiluminescence (ECL) detection system.

Immunofluorescence localisation

Living cells suspended in Pipes/HCl buffer (5 mM, pH 7.2) with KCl and $CaCl_2$ added (1 mM each) were exposed for up to 30 minutes to 0.01% saponin in the presence of $MgCl_2$, ATP-γ-S and NEM (1 mM each), in the same buffer solution. Then, when the cells were still viable, they were fixed at 22°C for 30 minutes in 8% formaldehyde (in phosphate-buffered saline, PBS) plus 0.1% Triton X-100, washed in PBS and then twice in PBS supplemented with 50 mM glycine, and finally in PBS plus bovine serum albumin (1%). Then they were exposed to anti-NSF Abs, followed by secondary Ab-FITC. In controls, the additives mentioned or primary Abs were omitted.

Electron microscopy and immunolabelling of ultrathin sections

PtNSF-silenced cells and non-silenced controls were treated identically as follows. For analysis of ultrastructural changes, cells were processed routinely (i.e. fixed in 2.5% glutaraldehyde, followed by 1% OsO_4, ethanol dehydration and embedding in Spurr's resin) and sections were sequentially stained with aqueous uranyl acetate followed by lead citrate at pH 12.0.

For immunolocalization, *PtNSF*-gene-silenced cells were fixed in 8% formaldehyde plus 0.1% glutaraldehyde (1 hour, 22°C) and then, for transportation, in 8% formaldehyde only, essentially as published (Flötenmeyer et al., 1999; Hauser et al., 2000). This combined formaldehyde/glutaraldehyde fixation protocol has been applied to allow for adequate fixation without too much loss of antigenicity. For the latter reason, glutaraldehyde had to be deleted during sample transport. We performed dehydration with ethanol by progressively lowering the temperature, followed by LR Gold embedding and UV polymerization at –35°C. After the usual washes, to avoid unspecific Ab binding, ultrathin sections were exposed to Abs (against PtNSF1-derived peptide, diluted 1:50) and then to protein A-Au$_{6nm}$ conjugate, followed by section staining with aqueous uranyl acetate only. EM micrographs of defined magnification collected from ~10 cell sections of each sample type were quantitatively evaluated by referring gold counts to area size analyzed, using the hit-point method (Plattner and Zingsheim, 1983). Then labeling density was normalized to cytoplasmic labeling.

Results

Cloning of the *Paramecium* NSF genes

A partial sequence resembling NSF, M09A04r, was found in a pilot genome project of *Paramecium* (Dessen et al., 2001; Sperling et al., 2002). In order to clone the full gene we took advantage of an indexed genomic library, with the aim to identify NSF-bearing clones in two hybridisation steps (Keller and Cohen, 2000), by using a probe designed from the sequence M09A04r (Fig. 1A). Nine clones were then retrieved, 5i21, 9a7, 20n10, 36e6, 63g7, 76m6, 105c22, 116p20 and 146k20. The positions of the *NSF* genes in the inserts were studied by restriction mapping and Southern blot analysis using the same probe. To see whether the inserts all contained the same *NSF* gene, a single-run sequencing was made with primer 9 on all of the nine clones. The clones displayed the same restriction map in the vicinity of the probe (except when the gene was at the border of the insert in clones 9a7, 36e6 and 63g7) and showed the same sequence over 400 bp. A single *NSF* gene was identified, *PtNSF1*. Clone 146k20, with the entire *PtNFS1* gene in the middle of a ~7 kb insert, was chosen for sequencing (accession number AJ347751).

After sequencing the complete *PtNSF1* gene, a second round of hybridisation of the indexed library was made with a probe corresponding to the entire ORF. In addition to the 9 clones previously identified with the short probe, three new ones were identified (50e4, 55e3 and 56o4), thus revealing a second gene, designated *PtNSF2*. A restriction mapping analysis showed that the three clones correspond to the same sequence, with
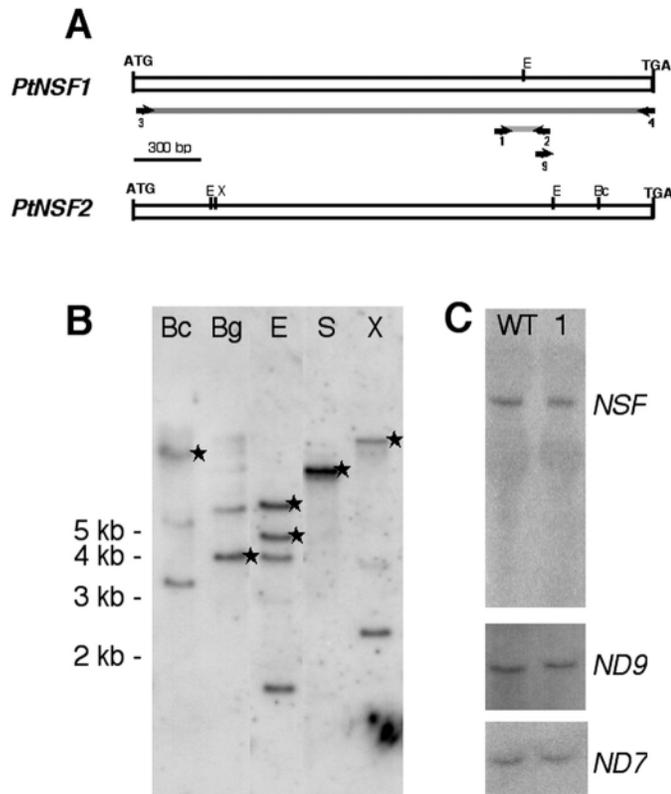
Fig. 1. *Paramecium NSF* genes. (A) Simplified restriction map of *PtNSF1* and *PtNSF2* genes and position of the probes and oligonucleotides used in this study. (B) Southern blot analysis of wild-type genomic DNA probed with the long probe (primers 3-4). A star marks the bands also revealed by the short probe (primers 1-2). Bc, *Bcl*I; Bg: *Bgl*II; E, *Eco*RV; S, *Swa*I; X, *Xba*I. (C) Northern blot analysis of total RNA from the wild-type (WT) and from the nd9-1 mutant (1) altered in the terminal step of exocytosis. Three probes were used, the long *PtNSF* probe, and, as controls, probes specific for the *ND9* and *ND7* genes (Froissard et al., 2001). By using the long *PtNSF* probe, a 2.3 kb band is revealed in both strains, with similar intensity.

are, respectively, 80, 64 and 83, suggesting that duplication occurred recently.

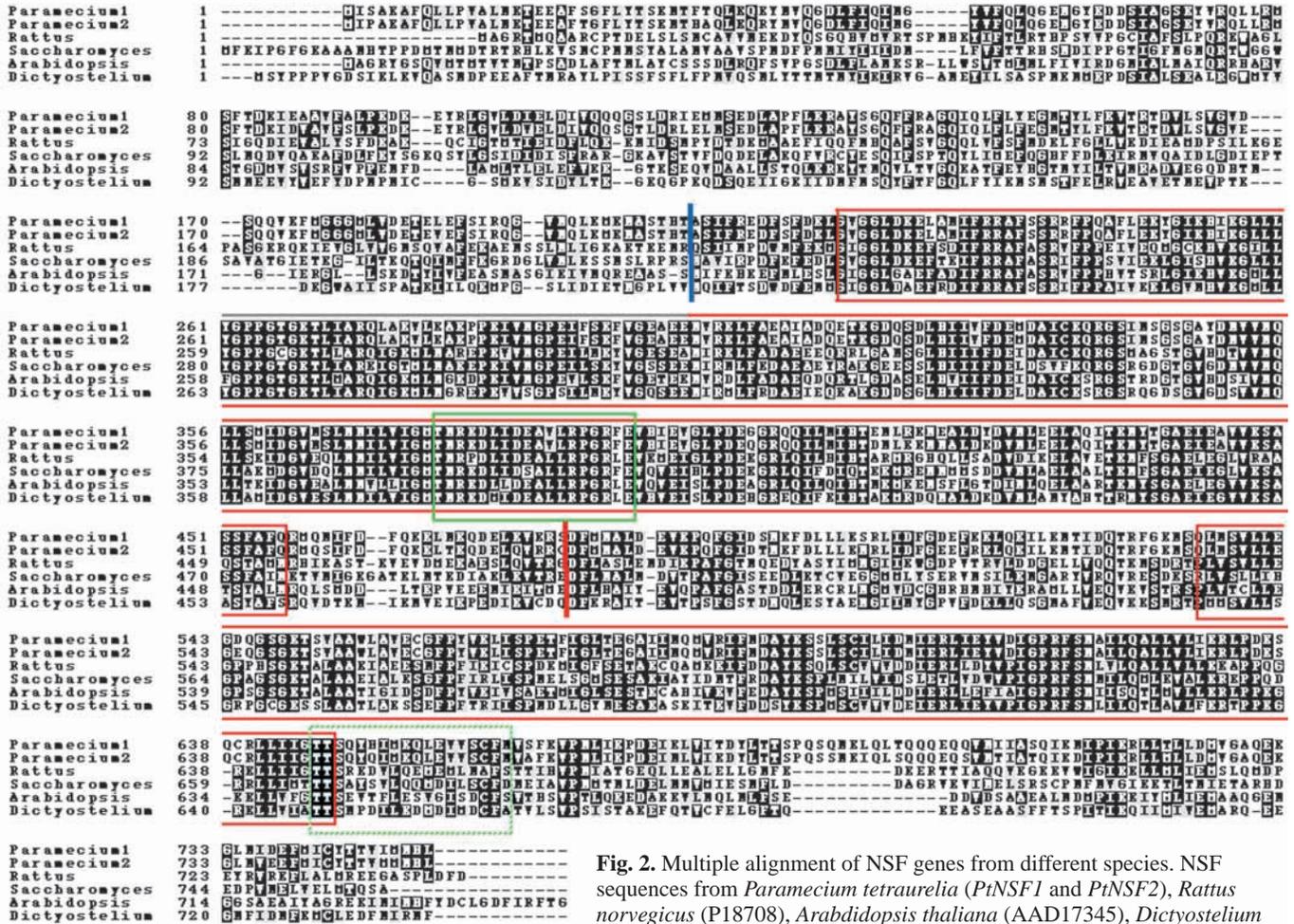## Characteristics and expression of the *Paramecium PtNSF* genes

The *PtNSF1* gene consisting of 2234 bp encodes a protein of 751 amino acids, with a calculated molecular weight of 84,671. The overall identities of its amino acid sequence with homologous genes from other species range from between 38.5% for *Drosophila melanogaster* and 42.1% for *Nicotiana tabacum*. In addition, the 2335 bp *PtNSF2* gene encodes a protein of 751 amino acids, with approximately the same calculated molecular weight (84,661) as *PtNSF1*. In the case of *PtNSF2* the overall identities at the amino acid level vary between 39.0% in *D. melanogaster* and 42.5% in *N. tabacum*.

PtNSF1 and *PtNSF2* genes are very similar, with ~87% identity at the nucleotide sequence level and ~93% at the protein sequence level. Sequence alignments with NSF proteins from other species revealed an average identity of ~40% throughout all kingdoms. Clearly, highest similarity occurs in functionally important domains (Fig. 2). Respective percentages of identity with *PtNSF1* and *PtNSF2* are: *Plasmodium falciparum* (a member of the closely related phylum Apicomplexa) (40.6/39.9); *Dicyostelium discoideum* (39.9/40.6); *Saccharomyces cerevisiae* (40.5/40.2); *D. melanogaster* (39.0/39.0 and 38.5/39.2 for *DmNSF1* and *DmNSF2*, respectively); *Arabidopsis thaliana* (40.7/41.3); and *Homo sapiens* (38.9/39.2). The alignment shows a very strong conservation over two-thirds of the molecule, particularly within the two blocks that interact with ATP, D1 and D2. As members of a large family of AAA-ATPases, the two *PtNSF* genes contain a 231 amino acid AAA domain centered in the Walker A and B boxes (Fig. 2). Similarities are particularly high for the functional domains, D1 and D2. Beyond this, they also contain the so-called second homology domain, which makes up part of the AAA cassette (Latterich, 1998). Owing to these signatures, there is no doubt that these genes encode PtNSF proteins.

The presence of the two genes in a cDNA library indicates that both isoforms are expressed. The expression level of *PtNSF1* and *PtNSF2* genes was also analyzed on northern blots by using the long probe, revealing a ~2.3 kb band (Fig. 1C), the size to be expected for both *PtNSF* transcripts.

Identification of PtNSF proteins

To identify and localize PtNSF proteins, we used either a crossreactive polyclonal Ab against NSF from yeast (affinity-purified IgGs against SEC18p) or a peptide-specific Ab against a unique sequence of *PtNSF1* located at the end of D1 (see Materials and Methods). The peptide selected for Ab production is remarkably different in NSF molecules from other species, when compared, for example, to the corresponding site 497-513 in *P. falciparum* or to 457-475 in *H. sapiens*. In western blots, the peptide used for immunization was therefore easily recognized by these Abs (data not shown), whereas no crossreactivity occurred when recombinant NSF from yeast Sec18p was used (Fig. 3, lane 9). However, with both types of Abs, anti-Sec18 Abs and anti-PtNSF1 Abs, we could detect PtNSF as a ~84 kDa band not only in whole cell

variable cloning position. Both extremities of the three inserts were sequenced. Clone 55e3 showed a sequence very similar to, but not identical to the 5′ sequence of *PtNSF1* close to the border of the insert. This plasmid was chosen for sequencing the entire *PtNSF2* gene (accession number AJ347752).

To look for any other possible *PtNSF* genes, Southern blot analysis on total genomic DNA revealed bands compatible with the restriction map of the clones containing *PtNSF1* when the short probe was used. Additional bands were observed with the long probe, in agreement with the restriction map obtained for the *PtNSF2* library clones (Fig. 1B). This suggests that only two *PtNSF* genes are present in the *Paramecium* genome.

The two *PtNSF* genes were also cloned from a *Paramecium* cDNA library, created from size-selected RNA (0.5-5 kb) of vegetative 51S cells (Klumpp et al., 1994). A comparison of the genomic sequences with their cDNA equivalents revealed that both genes contain three short introns at the same positions that all display the characteristics of *Paramecium*, bordered by 5′-GTA and TAG-3′ and of 25-28 nucleotides in size. The percentages of identity between the corresponding introns

Fig. 2. Multiple alignment of NSF genes from different species. NSF sequences from *Paramecium tetraurelia* (*PtNSF1* and *PtNSF2*), *Rattus norvegicus* (P18708), *Arabidopsis thaliana* (AAD17345), *Dictyostelium discoideum* (AAC48226) and *Saccharomyces cerevisiae* (AAA35031) were aligned using the CLUSTALW program and displayed using BOXSHADE. The conserved AAA domains of NSF ATPases are underlined. The Walker A and B domains (Patel and Latterich, 1998) are boxed in red. The limits between the N and D1, and D1 and D2 domains are indicated by vertical bars. An SRH domain is boxed in green and a divergent SRH domain is also boxed in green with dotted lines.

homogenates but also in particulate fractions enriched in ER (Fig. 3).

Silencing of *PtNSF* genes

Homology-dependent gene silencing can be efficiently obtained in *Paramecium* by microinjection into the macronucleus of large amounts of DNA corresponding to the coding sequence, without flanking 5′ and 3′ sequences (Ruiz et al., 1998; Bastin et al., 2001). We used the *PtNSF1* sequence, which is supposed to silence both *PtNSF* genes, since co-silencing is assumed for genes sharing ≥85% identity in nucleotide sequence [extrapolated from RNAi experiments in the nematode (Parrish et al., 2000) (see also Ruiz et al., 1998)].

After microinjection, cells underwent two fissions within 24 hours at 27°C, whereas controls made four fissions. Silenced cells displayed a characteristic phenotype: small size, dark appearance, decreasing motion rate. Whereas normal cells form approximately one digestive (food) vacuole per minute, silenced cells decreased and finally stopped phagocytosis activity. These criteria routinely served to identify silenced cells for subsequent analysis. Cells eventually died within 48

hours at 27°C. The defects we recognized after silencing were not simply general metabolic effects, since control experiments (e.g. with γ-tubulin silenced cells) showed quite different effects [i.e. they stopped duplicating their ciliary basal bodies and decreased their cell size after division (Ruiz et al., 1999)], whereas food vacuole formation was not affected (Froissard et al., 2002). All this indicates that silencing yields specific responses depending on the type of gene to be silenced.

We also found that the terminal step of stimulated trichocyst exocytosis is not affected in silenced cells. However, an effect of *PtNSF* silencing on the organization of microdomains in the exocytosis sites could be documented using a conditional mutant, nd9-1, in which this event could be decoupled from previous steps in trichocyst biogenesis (Froissard et al., 2002). Otherwise, *PtNSF* silencing has no effect on exocytosis sites, once they are established. On the EM level, *PtNSF*-silenced cells display massive changes, as documented in Fig. 4. The most salient changes are as follows. (1) Golgi fields increasingly disappear and become fragmented and ER cisternae swell (Fig. 4A,B). Owing to loss of ribosomes from ER in some places, it is not always possible to clearly identify the origin of each swollen cisterna, which may arise from ER,

Golgi, or endosomes, most of them localized in cortical regions (Allen, 1988). Frequently, many small transport vesicles appear attached, as though 'frozen', on such swollen cisternae, particularly in the cortex (Fig. 4A); they often look as though they were trapped after rounding up (Fig. 4B) but closure of such cisternae has not been shown since this would require serial sectioning. (2) Coated pits with clathrin [called 'parasomal sacs' in *Paramecium* (Allen, 1988; Allen et al., 1992)], if still present, may also appear 'frozen', sometimes in an atypical oblique attachment. Occasionally they are replaced by groups of smooth vesicles (Fig. 4C). (3) Early endosomes ['terminal cisternae' (Patterson, 1978; Allen, 1988)] either appear swollen or are totally missing (Fig. 4A). Since both these structures may serve constitutive exo-/endocytosis
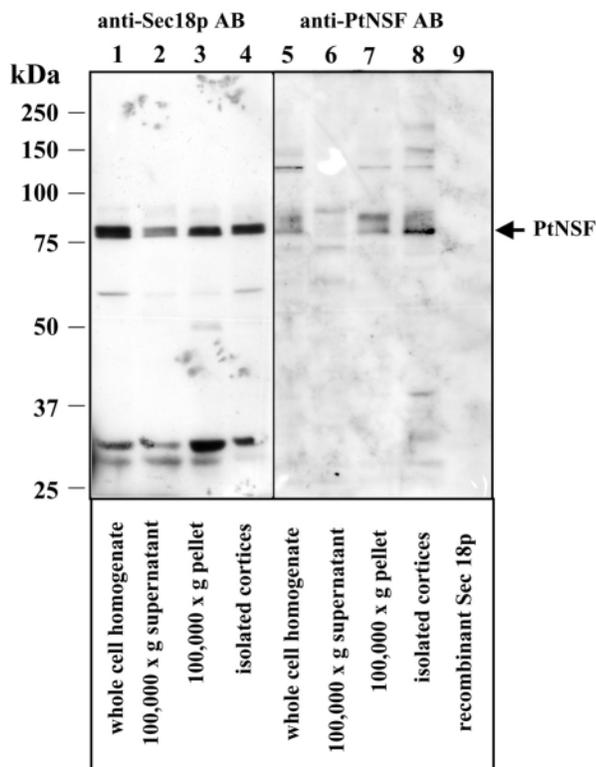
Fig. 3. Western-blot analysis of the subcellular distribution of PtNSF using affinity-purified Abs against yeast and *Paramecium* NSF. Aliquots of 50 μg of whole cell homogenates (lanes 1,5), 100,000 *g* supernatant (lanes 2,6), 100,000 *g* pellet (lanes 3,7), isolated cortices (lanes 4,8), and of 100 ng of recombinant Sec18p (lane 9) were separated on a 10% SDS polyacrylamide gel and electroblotted onto nitrocellulose membranes. Immunoreactions were carried out with either affinity-purified and crossreactive polyclonal Abs against Sec18p (lanes 1-4) (Mayer et al., 1996) or with affinity-purified peptide-specific Abs against PtNSF1 (lanes 5-9), as described in the Materials and Methods. Note that each of the two Abs immunoreact with a protein band at ~84 kDa (arrow) not only in whole cell homogenates but also in particulate fractions rich of ER. In addition, the polyclonal Ab against SEC18p (anti-yeast NSF) also recognizes some bands at ~30 kDa (lanes 1-4), which might be the result of proteolytic activity or instability of the NSF protein itself. By using the peptide-specific Ab against *Paramecium* PtNSF, some higher molecular weight bands are also reactive, which may represent heteromeric complexes of NSF, which still have to be analysed in more detail.

(Flötenmeyer et al., 1999), our observations imply disturbance of these processes. (4) Furthermore, phagocytosis is increasingly depressed in the course of NSF silencing (a criterion of successful silencing), as is (5) the formation and/or transport of discoidal vesicles (not shown), which normally serve membrane recycling, after defecation from spent vacuoles to the site of the formation of new phagosomes (Allen et al., 1995; Allen and Fok, 2000). (6) Aggregates of small vesicles sticking together around fields of ER (with intense gold labeling, as shown in Fig. 6D) occur at different sites (Fig. 4D), whereas they are absent in non-silenced cells. These regions contain ribosomes, thus strongly suggesting their origin from ER (Fig. 4D). Such forms of ER are known to occur in *Paramecium* (Allen, 1988; Fok and Allen, 1981). Identification of ER-related structures is supported by the higher magnification of Fig. 6D in Fig. 6E.

Silencing experiments may also reveal biogenetic pathways, when transport vesicles are 'frozen' firmly attached at a target membrane (Fig. 4C, Fig. 5). This had to be expected for the interaction of small vesicles with phagosomal membranes (Allen and Fok, 1984) since different types of vesicles bud and fuse during their life cycle. However, we see for the first time occasional attachment of small vesicles, ~30 nm in diameter, at alveolar sacs, which may support their biogenesis via vesicle flow, as discussed below.

Immunolabeling

Immuno-gold labeling data obtained by anti-PtNSF Abs after *PtNSF* gene silencing are presented in Fig. 6A,B and Table 1. It is not easy on such sections to discriminate between ER and Golgi areas (owing to low contrast allowed by the fixation method) and different types of small vesicles scattered in such ER-rich domains, which therefore are taken as representative for general cytoplasmic labeling. (In non-silenced cells, these domains are homogenously labeled; Fig. 6C.) The low values, with large s.e.m., found over trichocysts and lipid droplets are not statistically significant. However, in silenced cells, lysosomes (identified by their size of ~1 μm, compact contents and single membrane envelope) are slightly but significantly labeled (Table 1). This indicates ongoing degradation of PtNSF molecules, while formation of new ones is inhibited, which results in the decrease in vesicle traffic described above. Concomitantly, aggregates, several microns in size, of intimately clumped cisternae occur (compare Fig. 6A,B with Fig. 4D). Since they are 4.75-times more labeled than the average cytoplasm (Table 1), this may indicate inability to

Table 1. Immunolocalization of PtNSF using peptide-specific Abs against PtNSF

	Cytoplasm (mainly ER)	Vesicle aggregates	Lysosomes	Background over:	
				trichocysts	lipid droplets
Labeling density	100.0%	471.3%	44.0%	12.0	13.9
±s.e.m.	±11.0	±96.6	±8.4	±5.1	±7.2

Labeling densities based on gold grain counts (protein A-Au$_{6nm}$ conjugates per unit area size), normalized to values determined in the cytoplasm (100.0%=59.3 Au$_6$-particles. μm^{-2}) after off-cell background subtraction.
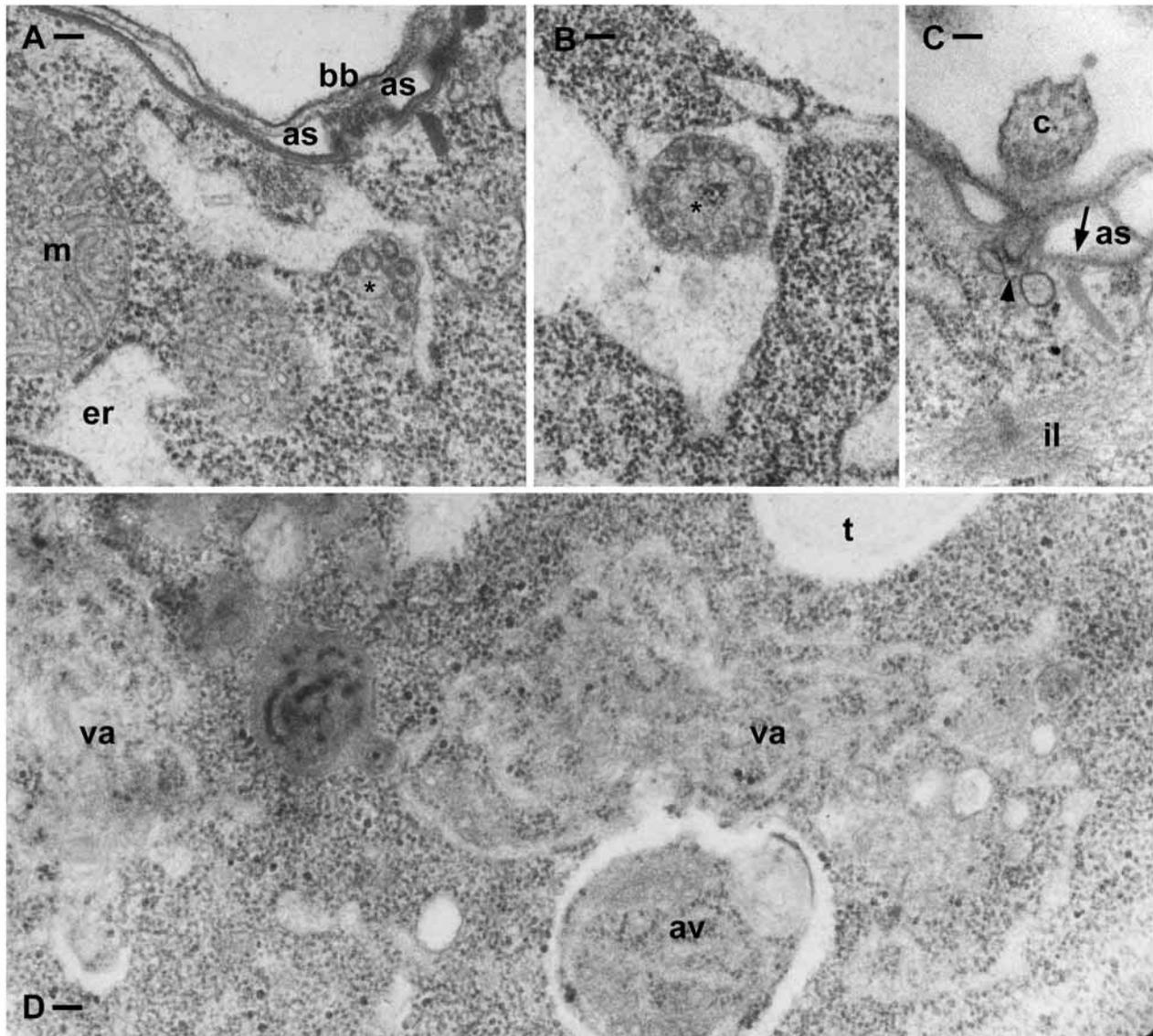
Fig. 4. Ultrastructural changes caused by *PtNSF* gene silencing (A-D). Panel A shows a dilated cortical cisterna, located below a ciliary basal body (bb) and flanked by alveolar sacs (as), with locally attached ~0.05 μm large vesicles (asterisk). Some attached ribosomes indicate its possible origin from endoplasmic reticulum, which is frequently swollen (er, lower left). The 'terminal cisterna' (early endosome) normally expected below a basal body is absent. (B) A structure similar to that seen in A has rounded-up and closed to a wheel-like structure with vesicles firmly attached at the cytosolic site trapped inside (asterisk). (C) Close to the emergence of a cilium (c), here in oblique section, at the site where alveolar sacs are interrupted, vesicles occur, instead of the usual single 'parasomal sac' (clathrin-coated pit/vesicle). The arrow points to a very slim vesicle approaching the inner side of an alveolar sac (a similar vesicle can be detected in A and more are seen in Fig. 5B). The 'infraciliary lattice' (il) made up of filamentous structures is unchanged. (D) Note accumulation of clumped vesicular ER elements (va; corresponding to densely immunolabeled cytoplasmic zones in Fig. 6A,B), largely devoid of ribosomes, the occurrence of numerous free ribosomes outside such vesicle aggregates and of an autophagic vacuole (av). m, mitochondria; t, trichocyst. Bars, 0.1 μm.

dissociate SNARE complexes and to drive vesicle transport and fusion at this stage of silencing. Reduced vesicle traffic may, thus, also explain decreasing cell size during NSF gene silencing.

To increase the chance of seeing PtNSF bound as a complex to target membranes, we used NSF ATPase activity inhibitors such as ATP-γ-S and NEM in immunofluorescence experiments. Cells were carefully permeabilized and association of PtNSF with fusogenic sites was maintained by adding the inhibitors, followed by immuno-FITC labeling.

This resulted in labeling of the cytostome and cytoproct region (Fig. 7A,B), of the outlets of contractile vacuoles (Fig. 7B), and of the onsets of radial canals, as shown in Fig. 7B,C. Different labeling intensity of these sites with periodic membrane (dis-)connection may indicate some asynchrony in their membrane-to-membrane interaction. In control cells, subjected to the labeling protocol without ATP-γ-S and NEM (or without primary Ab), these structures were not labeled (Fig. 7E,F). These data further support specificity of Ab binding, since anti-PtNSF Abs bind to specific sites only when
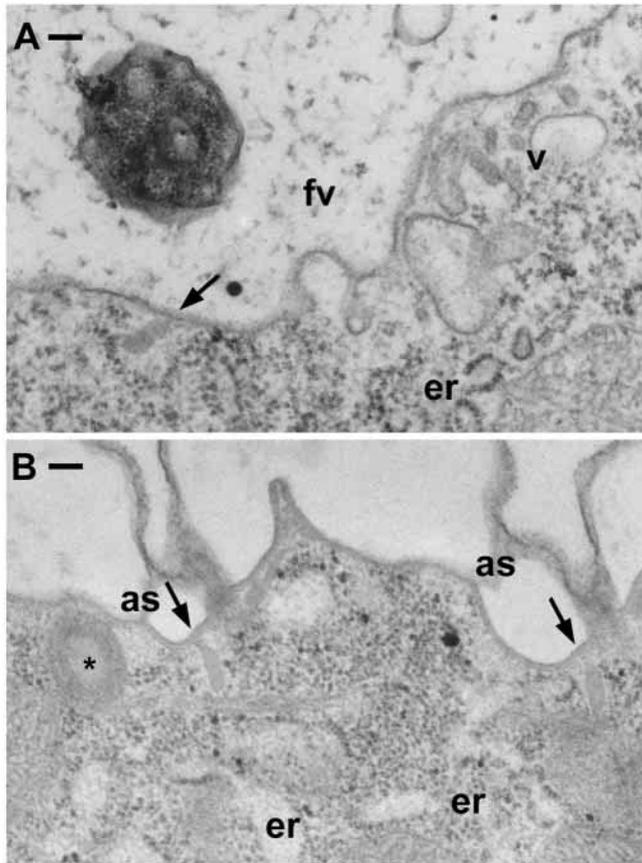
Fig. 5. After *PtNSF* gene silencing, docking of slender vesicles of similar appearance is seen on a food vacuole membrane in A and at alveolar sacs in B. The type of vesicles highlighted by arrows, only rarely seen on food vacuoles (fv), has never been observed previously on the inner membrane of alveolar sacs (as) to whose biogenesis it may contribute. er, endoplasmic reticulum; v, vesicle. Bars, 0.1 µm.

Table 2. Involvement of PtNSF in membrane traffic pathways of *Paramecium tetraurelia*

Phenotypic changes in PtNSF-silenced cells

Observations in vivo

Decreased cell size	Reduced/abolished phagocytosis activity
Slow swimming	Eventually cell death within 48 hours

Observations on the subcellular level

ER swelling	Absence or fragmentation of Golgi apparatus

'Frozen' parasomal sacs (see text) with atypical oblique attachment
Reduced early endosome formation
Reduced phagocytosis
Reduced formation and transport of discoidal vesicles
'Minivesicles' attached to large food vacuoles,
'Minivesicles' attached to the inner region of alveolar membranes

Immunofluorescence locations of PtNSF (in permeabilized cells under conditions of NSF retention: ATP-γ-S and NEM)

Cytostomal region
Cytoproct region
Outlets of contractile vacuoles
Attachements of radial canals to contractile vacuoles

In this work, we identified and studied two *NSF* genes in *Paramecium*. We combined cytological and ultrastructural studies with gene silencing experiments to gain insight into the function and site of action of NSF. To localize PtNSF in situ, we used anti-NSF Abs in conjunction with gold-labeling after silencing, and Ab-fluorescence labeling in normal cells. Thereby we took into account that PtNSF may be trapped at membrane-to-membrane interaction zones if its rapid dissociation after SNARE assembly is blocked by inhibiting its ATPase activity. Our approach was greatly facilitated by the occurrence of well established avenues of vesicle traffic in *Paramecium*. Together, we showed that PtNSF is involved in most, if not all, membrane traffic pathways recognizable in *Paramecium*. This is the first experimental evidence that, in these pathways, complex NSF/SNAP/SNARE machinery must operate, as is the case in other eukaryotes.
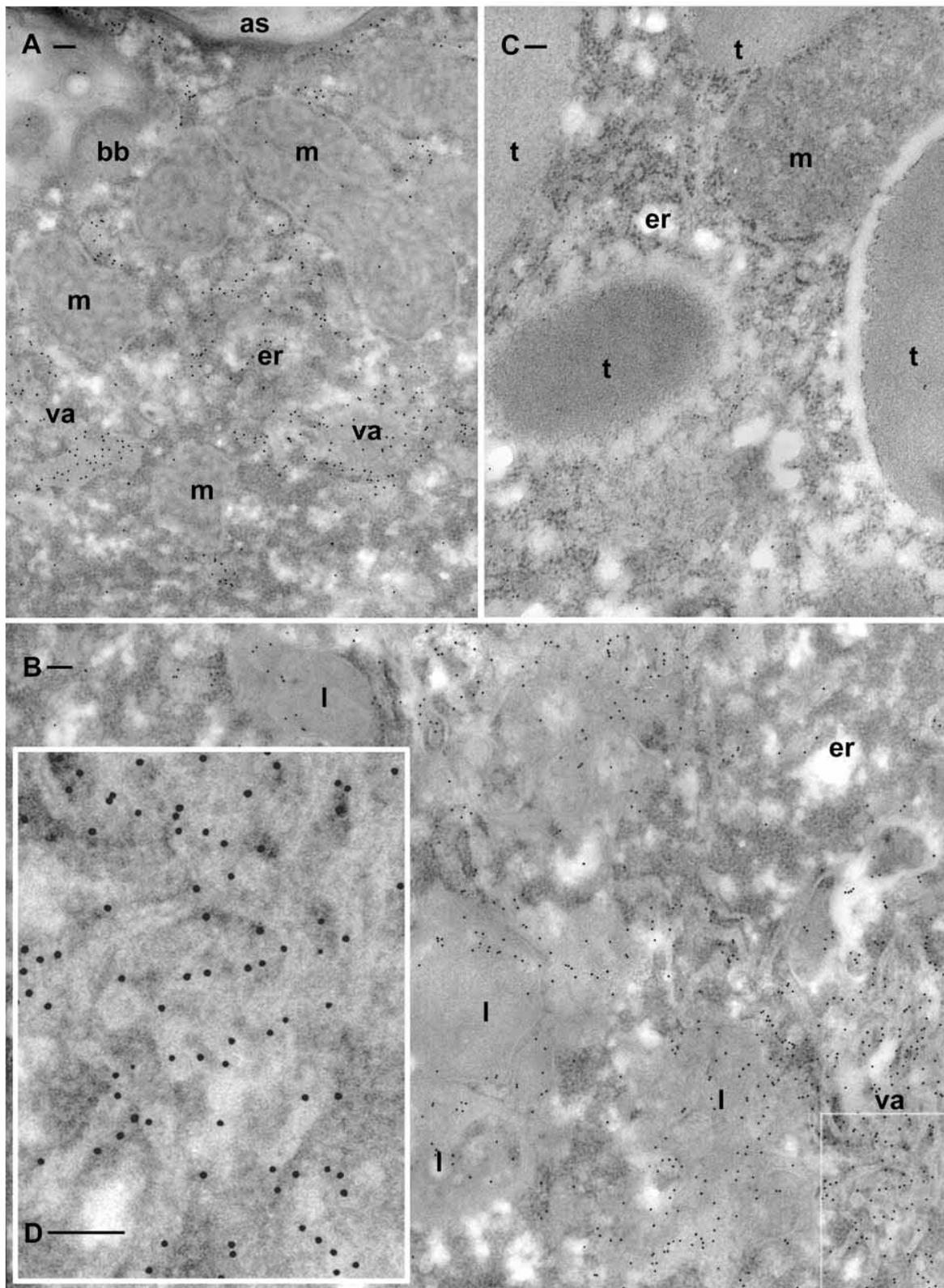
Two closely related NSF genes in *Paramecium*

The two *PtNSF* genes found have 87% nucleotide identity, each gene encoding a protein of 84.7 kDa with 94% identity. The occurrence of at least two expressed genes for the same kind of protein is frequent in *P. tetraurelia* (Hauser et al., 1997; Bernhard and Schlegel, 1998; Kim et al., 1998; Chan et al., 1999).

The reason why *Paramecium* expresses two rather similar *NSF* genes remains unclear. Searches in the *Caenorhabditis elegans* and the human genome databases reveal only one *NSF* gene, indicating that a single *NSF* gene can support all membrane traffic. In rats, NSF transcripts undergo alternative splicing (Puschel et al., 1994). In *D. melanogaster,* which possesses two *NSF* genes (Ordway et al., 1994; Pallanck et al., 1995), the two are expressed at different stages of development, despite similar functional properties (Golby et al., 2001).

Effects of NSF gene silencing

The close resemblance of the two *PtNSF* genes in *Paramecium* suggests that gene silencing experiments on one gene affect

cautiously permeabilized cells were exposed to conditions mediating irreversible NSF binding to potential fusion sites. Beyond that, requirement of ATP for detachment of NSF from membranes can also explain why a high percentage of PtNSF is membrane-bound in western blots from cell fractions (Fig. 3).

Discussion

All eukaryotic cells are made of membrane-bounded compartments, whose biogenesis and interplay is orchestrated by a complex membrane traffic involving vesicle budding from donor compartments and fusion with target membranes. As a highly differentiated cell, *Paramecium* displays numerous co-existing membrane traffic pathways to fulfill its various cellular functions, including endocytosis, phagocytosis, regulated exocytosis of trichocysts and constitutive exocytosis, the latter including discharge of spent food vacuole contents and of contractile vacuole fluid. NSF is a protein central to membrane fusion and recycling so that its identification in association with a particular compartment/pathway is a signature of membrane recognition, docking and fusion events.

Fig. 6. EM immuno-gold localization of PtNSF in gene-silenced (A,B,D) and control cells (C) using peptide-specific Abs against PtNSF. Note the irregular distribution of label in the cytoplasmic zones enriched in endoplasmic reticulum (er) (A,B,D), in contrast to the control (C) with rather homogenously distributed gold grains in the cytoplasm. In all cases (A-D), mitochondria (m), trichocysts (t), alveolar sacs (as) and ciliary basal bodies (bb) are essentially devoid of label. In A and B, silencing has produced the accumulation of densely labeled vesicle aggregates (va), whose morphology is more clearly identified, probably as clusters of branching ER, in panel D, which shows a higher magnification of the area marked in the lower right corner of B. Some label also occurs in bona fide lysosomes (l). Bars, 0.1 μm.

both genes. However, it is not excluded that only *PtNSF1* is silenced and not *PtNSF2*. In this case, this would mean that *PtNSF1* by itself is (1) essential and (2) not replaceable by *PtNSF2*.

Silencing of the *PtNSF* genes has a dramatic influence not only on the growth and survival of clonal descendants, but also on their subcellular organization (Table 2). Different types of vesicle transport operate at different rates and, therefore, may have a different sensitivity to *PtNSF* silencing. According to our EM analysis, rough ER-to-Golgi delivery, early endosome formation, and recycling of spent phagosomal membranes from the cytoproct to the cytostome via discoidal vesicles, appear very sensitive to NSF deprivation. Concomitantly, these structures either undergo deformation or disappear. *NSF* gene knockout in yeast also disturbs ER to Golgi vesicle delivery (Graham and Emr, 1991) and endocytotic vesicle trafficking (Prescianotto-Baschong and Riezman, 1998). In contrast, exocytosis of docked trichocysts can be triggered in a normal manner in *PtNSF*-silenced cells. This may imply that the sensitivity of an organelle to silencing may depend on the turnover of intermembrane interactions. Once trichocysts are attached to the plasma membrane, the situation is rather stable and requires no further rounds of PtNSF interaction.

After *PtNSF* silencing, many of the transport vesicles clump together to form big aggregates, just as in yeast after *NSF* gene knockout (Novick et al., 1980). As we show, such vesicle aggregates are most heavily labeled with anti-NSF Ab-gold conjugates. Some label clearly above general cytoplasmic labeling, specifically of ER-rich zones, but well below that in vesicle aggregates, also occurs in lysososmes, identified by their size, shape and appearance of their contents. Later, lysosomal enzyme delivery and/or retrieval from phagosomes (Allen and Fok, 2000) may also be interrupted. Accordingly, some phago-lysosomes show unusual numbers of small vesicles attached after silencing. Both the clustering of strongly labeled small vesicles in some areas of silenced cells and the ongoing deformation of some of the organelles participating in membrane traffic indicate increasing abolition of vesicle traffic. Clearly the osmoregulatory system functions longer than the phagocytotic pathway, possibly because it requires far fewer membrane fusion events (Allen, 2000), in contrast to the multiple rounds of fusion events, each involving a multitude of vesicles (acidosomal, discoidal, primary lysosomal, endocytotic), required during a digestive cycle (Allen and Fok, 2000).
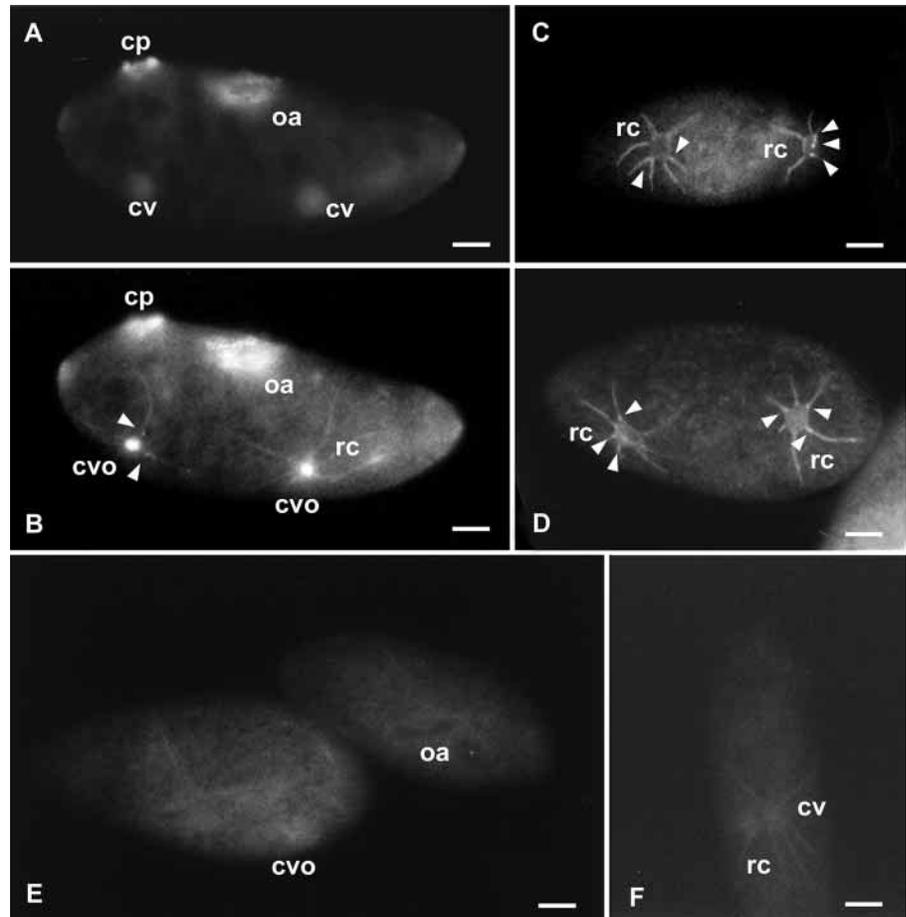
Fig. 7. Anti-NSF Ab-fluorescence labeling of normal cells. Live cells were carefully permeabilized with saponin in the presence (A-D) or absence (E,F; controls) of ATP-γ-S and NEM, fixed in formaldehyde, with Triton X-100 added for complete permeabilization, followed by anti-PtNSF Ab labeling, as outlined in Materials and Methods. In panels A-D several structures known to undergo multiple or individual vesicle fusions are labeled (for details, see text), for example, oral apparatus (oa), cytoproct (cp), outlets (cvo) of contractile vacuoles (cv) and onsets (arrowheads) of radial canals (rc) on these vacuoles, shown with variable labeling in different stages. In controls (E,F, without additives), the outlines of some of these structures can be vaguely seen with some residual fluorescence. Bars, 10 μm.

Rare fusion events are trapped by inhibiting NSF dissociation

To visualize PtNSF at the whole cell level, we took advantage of the general property of NSF to dissociate from the SNARE complex upon ATP hydrolysis (Whiteheart et al., 2001). We then developed a new protocol to visualize potential membrane fusion zones by NSF Ab-fluorescence labeling. This includes careful saponin permeabilization of viable cells in the presence of ATP-γ-S and NEM, to block PtNSF dissociation from membrane attachment/fusion sites. The outcome was uncertain a priori for the following reason. On the one hand, in addition to ATPase activity, an additional role had been assigned to NSF in SNARE (dis-)assembly (Müller et al., 1999). On the other hand, a requirement of ATP in in vitro SNARE disassembly had recently been shown (Wagner et al., 2001). With our approach, we could clearly label low frequency docking zones under restrictive conditions. Not only are the cytostome, the cytoproct and the outlet of the contractile vacuole labeled, but also the attachments

of radial canals to the contractile vacuole. Their repeated disconnection and reconnection during activity cycles has been a matter of debate (Hausmann and Allen, 1977). Our data agree with the more recent indirect evidence from electrophysiological recordings (Tominaga et al., 1998a; Tominaga et al., 1998b). Even occasional labeling of radial canals and of the attached spongiome membranes would fit the eventual vesiculation and refusion of these membranes, as reported previously (Tominaga et al., 1998b). Some of the ubiquitous vacuoles and vesicles of different sizes, which are also labeled, are more difficult to identify – they are probably components of different origin of the elaborate endo-/phago-/lysosomal system. This is even more difficult for the widely branching bulk of ER components, with the numerous Golgi fields in-between. In agreement with EM labeling analysis, the firmly established docking sites of trichocysts are not labeled by this procedure.

Unexpected aspects of organelle biogenesis

Membrane biogenesis frequently operates very inconspicuously and, therefore, may not always be evident from EM micrographs. However, when halted by *PtNSF* silencing, attachment of small vesicles can indicate such biogenetic pathways. We show this first for digestive vacuoles for which such a pathway is established (Allen and Fok, 2000), but then also for alveolar sacs, whose biogenesis was under considerable debate until recently (Capdeville et al., 1993; Flötenmeyer et al., 1999). After *PtNSF* gene silencing, ~30 nm wide vesicles are occasionally seen attached to alveolar sacs. Recently, both expression of an ER-type Ca^{2+}-ATPase (pump) as a fusion protein with green fluorescent protein and staining by affinity probes in vivo have suggested a biogenetic pathway by vesicle flow in *Paramecium* (Hauser et al., 2000). However, it was previously difficult to imagine how even small vesicles could reach alveolar sacs since their side facing the cell center is lined by an electron dense epiplasmic layer.

Conclusions

Paramecium is an ideal single cell system for numerous types of experiments, and studies such as those presented here are needed to ensure that our understanding of this system will keep pace with knowledge of membrane trafficking systems in multicellular organisms. Beyond the existence of NSF and the description of NSF-dependent processes in *Paramecium*, this work may also reveal how to look for SNAREs and other partners of NSF and the SNARE machinery. Combined with the extensive genetic and molecular study of the multiple, well-defined secretory pathways in *Paramecium*, a biochemical approach will help to unravel the specificity of the components mediating interaction of the respective membranes and the mechanisms of their membrane fusion.

References

Allen, R. D. (1988). Cytology. In *Paramecium* (ed. H. D. Görtz,), pp. 4-40. Berlin, Heidelberg, New York: Springer-Verlag.

Allen, R. D. (2000). The contractile vacuole and its membrane dynamics. *BioEssays* **22**, 1035-1042.

Allen, R. D. and Fok, A. K. (1984). Retrieval of lysosomal membrane and acid phosphatase from phagolysosomes of *Paramecium caudatum*. *J. Cell Biol.* **99**, 1955-1959.

Allen, R. D. and Fok, A. K. (2000). Membrane trafficking and processing in *Paramecium*. *Int. Rev. Cytol.* **198**, 277-317.

Allen, R. D., Schroeder, C. C. and Fok, A. K. (1992). Endosomal system of *Paramecium*: coated pits to early endosomes. *J. Cell Sci.* **101**, 449-461.

Allen, R. D., Bala, N. P., Ali, R. F., Nishida, D. M., Aihara, M. S., Ishida, M. and Fok, A. K. (1995). Rapid bulk replacement of acceptor membrane by donor membrane during phagosome to phagoacidosome transformation in *Paramecium*. *J. Cell Sci.* **108**, 1263-1274.

Augustine, G. J., Burns, M. E., DeBello, W. M., Hilfiker, S., Morgan, J. R., Schweizer, F. E., Tokumaru, H. and Umayahara, K. (1999). Proteins involved in synaptic vesicle trafficking. *J. Physiol.* **520**, 33-41.

Bastin, P., Galvani, A. and Sperling, L. (2001). Genetic interference in protozoa. *Res. Microbiol.* **152**, 123-129.

Bernhard, D. and Schlegel, M. (1998). Evolution of histone H4 and H3 genes in different ciliate lineages. *J. Mol. Evol.* **46**, 344-354.

Bradford, M. M. (1976). A rapid and sensitive method for the quantitation of microgram quantities of protein utilizing the principle of protein-dye binding. *Anal. Biochem.* **72**, 248-254.

Capdeville, Y., Charret, R., Antony, C., Delorme, J., Nahon, P. and Adoutte, A. (1993). Ciliary and plasma membrane proteins in *Paramecium*: description, localization, and intracellular transit. In *Membrane Traffic in Protozoa* (ed. H. Plattner), pp. 181-226. Greenwich, CT, USA, London, UK: JAI Press.

Chan, C. W., Saimi, Y. and Kung, C. (1999). A new multigene family encoding calcium-dependent calmodulin-binding membrane proteins of *Paramecium tetraurelia*. *Gene* **231**, 21-32.

Chomczynski, P. and Sacchi, N. (1987). Single-step method of RNA isolation by acid guanidinium thiocyanate-phenol-chloroform extraction. *Anal. Biochem.* **162**, 156-159.

Church, G. M. and Gilbert, W. (1984). Genomic sequencing. *Proc. Natl. Acad. Sci. USA* **81**, 1991-1995.

Dessen, P., Zagulski, M., Gromadka, R., Plattner, H., Kissmehl, R., Meyer, E., Bétermier, M., Schultz, J., Linder, J., Pearlman, R. et al. (2001). *Paramecium* genome survey: a pilot project. *Trends Genet.* **17**, 306-308.

Duharcourt, S., Butler, A. and Meyer, E. (1995). Epigenetic self-regulation of developmental excision of an internal eliminated sequence on *Paramecium tetraurelia*. *Genes Dev.* **9**, 2065-2077.

Flötenmeyer, M., Momayezi, M. and Plattner, H. (1999). Immunolabeling analysis of biosynthetic and degradative pathways of cell surface components (glycocalyx) in *Paramecium* cells. *Eur. J. Cell Biol.* **78**, 67-77.

Fok, A. K. and Allen, R. D. (1981). Axenic *Paramecium caudatum*. II. Change in fine structure with culture age. *Eur. J. Cell Biol.* **25**, 182-192.

Froissard, M., Keller, A. and Cohen, J. (2001). ND9p, a novel protein with *armadillo*-like repeats involved in exocytosis: physiological studies using allelic mutants in *Paramecium*. *Genetics* **157**, 611-620.

Froissard, M., Kissmehl, R., Dedieu, J.-C., Gulik-Krzywicki, T., Plattner, H. and Cohen, J. (2002). NSF is required to organize functional exocytotic microdomains in *Paramecium*. *Genetics* **161**, 643-650.

Galvani, A. and Sperling, L. (2001). Transgene-mediated post-transcriptional gene silencing is inhibited by 3′ non-coding sequences in *Paramecium*. *Nucleic Acids Res.* **29**, 4387-4394.

Gautier, M. C., Garreau de Loubresse, N., Madeddu, L. and Sperling, L. (1994). Evidence for defects in membrane traffic in *Paramecium* secretory mutants unable to produce functional storage granules. *J. Cell Biol.* **124**, 893-902.

Golby, J. A., Tolar, L. A. and Pallanck, L. (2001). Partitioning of N-ethylmaleimide-sensitive fusion (NSF) protein function in *Drosophila melanogaster*: dNSF1 is required in the nervous system, and dNSF2 is required in mesoderm. *Genetics* **158**, 265-278.

Graham, T. R. and Emr, S. D. (1991). Compartmental organization of Golgi-specific protein modification and vacuolar protein sorting events defined in a yeast sec18 (NSF) mutant. *J. Cell Biol.* **114**, 207-218.

Hanson, P., Roth, R., Morisaki, H., Jahn, R. and Heuser, J. (1997). Structure and conformational changes in NSF and its membrane receptor

complexes visualized by quick-freeze/deep-etch electron microscopy. *Cell* **90**, 523-535.

Hauser, K., Kissmehl, R., Linder, J., Schultz, J. E., Lottspeich, F. and Plattner, H. (1997). Identification of isoforms of the exocytosis-sensitive phosphoprotein PP63/parafusin in *Paramecium tetraurelia* and demonstration of phosphoglucomutase activity. *Biochem. J.* **323**, 289-296.

Hauser, K., Pavlovic, N., Kissmehl, R. and Plattner, H. (1998). Molecular characterization of a sarco(endo) plasmic reticulum Ca^{2+}-ATPase gene from *Paramecium tetraurelia* and localization of its gene product. *Biochem. J.* **334**, 31-38.

Hauser, K., Pavlovic, N., Klauke, N., Geissinger, D. and Plattner, H. (2000). Green fluorescent protein-tagged sarco(endo)plasmic reticulum Ca^{2+}-ATPase overexpression in *Paramecium* cells: isoforms, subcellular localization, biogenesis of cortical calcium stores and functional aspects. *Mol. Microbiol.* **37**, 773-787.

Hausmann, K. and Allen, R. D. (1977). Membranes and microtubules of the excretory apparatus of *Paramecium caudatum*. *Cytobiologie* **15**, 303-320.

Jahn, R. and Südhof, T. C. (1999). Membrane fusion and exocytosis. *Annu. Rev. Biochem.* **68**, 863-911.

Kaneshiro, E. S., Beischel, L. S., Merkel, S. J. and Rhoads, D. E. (1979). The fatty acid composition of *Paramecium aurelia* cells and cilia: changes with culture age. *J. Protozool.* **26**, 147-158.

Keller, A.-M. and Cohen, J. (2000). An indexed genomic library for *Paramecium* complementation cloning. *J. Eukaryot. Microbiol.* **47**, 1-6.

Kim, K., Messinger, L. A. and Nelson, D. L. (1998). Ca^{2+}-dependent protein kinases of *Paramecium*. Cloning provides evidence of a multigene family. *Eur. J. Biochem.* **251**, 605-612.

Kissmehl, R., Treptau, T., Kottwitz, B. and Plattner, H. (1997). Occurrence of a para-nitrophenyl phosphate-phosphatase with calcineurin-like characteristics in *Paramecium tetraurelia*. *Arch. Biochem. Biophys.* **344**, 260-270.

Kissmehl, R., Hauser, K., Gössringer, M., Momayezi, M., Klauke, N. and Plattner, H. (1998). Immunolocalization of the exocytosis-sensitive phosphoprotein, PP63/parafusin, in *Paramecium* cells using antibodies against recombinant protein. *Histochem. Cell Biol.* **110**, 1-8.

Klumpp, S., Hanke, C., Donella-Deana, A., Beyer, A., Kellner, R., Pinna, L. A. and Schultz, J. E. (1994). A membrane-bound protein phosphatase type 2C from *Paramecium tetraurelia*. Purification, characterization, and cloning. *J. Biol. Chem.* **269**, 32774-32780.

Laemmli, U. K. (1970). Cleavage of structural proteins during the assembly of the head of bacteriophage T4. *Nature* **227**, 680-685.

Latterich, P. S. (1998). The AAA team: related ATPases with diverse functions. *Trends Cell Biol.* **8**, 65-71.

May, A. P., Whiteheart, S. W. and Weis, W. I. (2001). Unraveling the mechanism of the vesicle transport ATPase NSF, the N-ethylmaleimide-sensitive factor. *J. Biol. Chem.* **276**, 21991-21994.

Mayer, A., Wickner, W. and Haas, A. (1996). Sec18p (NSF)-driven release of sec17p (alpha-SNAP) can precede docking and fusion of yeast vacuoles. *Cell* **85**, 83-94.

Momayezi, M., Habermann, A. W., Sokolova, J. J., Kissmehl, R. and Plattner, H. (1993). Ultrastructural and antigenic preservation of a delicate structure by cryopreparation: Identification and immunogold localization during biogenesis of a secretory component (membrane-matrix connection) in *Paramecium* trichocysts. *J. Histochem. Cytochem.* **41**, 1669-1677.

Morgan, A. and Burgoyne, R. D. (1995). Is NSF a fusion protein? *Trends Cell Biol.* **5**, 335-339.

Müller, J. M. M., Rabouille, C., Newman, R., Shorter, J., Freemont, P., Schiavo, G., Warren, G. and Shima, D. T. (1999). An NSF function distinct from ATPase-dependent SNARE disassembly is essential for Golgi membrane fusion. *Nat. Cell Biol.* **1**, 335-340.

Neuwald, A. F., Aravind, L., Spouge, J. L. and Koonin, E. V. (1999). AAA+: A class of chaperone-like ATPases associated with the assembly, operation, and disassembly of protein complexes. *Genome Res.* **9**, 27-43.

Novick, P., Field, C. and Schekman, R. (1980). Identification of 23 complementation groups required for post-translational events in the yeast secretory pathway. *Cell* **21**, 205-215.

Ordway, R. W., Pallanck, L. and Ganetzky, B. (1994). Neurally expressed *Drosophila* genes encoding homologs of the NSF and SNAP secretory proteins. *Proc. Natl. Acad. Sci. USA* **91**, 5715-5719.

Owen, D. J. and Schiavo, G. (1999). A handle on NSF. *Nat. Cell Biol.* **1**, E127-E128.

Pallanck, L., Ordway, R. W., Ramaswami, M., Chi, W. Y., Krishnan, K.
S. and Ganetzky, B. (1995). Distinct roles for N-ethylmaleimide-sensitive fusion protein (NSF) suggested by the identification of a second *Drosophila* NSF homolog. *J. Biol. Chem.* **270**, 18742-18744.

Patel, S. and Latterich, M. (1998). The AAA team: relaed ATPases with diverse functions. *Trends Cell Biol.* **8**, 65-71

Parrish, S., Fleenor, J., Xu, S., Mello, C. and Fire, A. (2000). Functional anatomy of a dsRNA trigger: differential requirement for the two trigger strands in RNA interference. *Mol. Cell* **6**, 1077-1087.

Patterson, D. J. (1978). Membranous sacs associated with cilia of *Paramecium*. *Cytobiologie* **17**, 107-113.

Plattner, H. (1993). Membrane traffic. In *Protozoa* (ed. H. Plattner). Greenwich, CT, USA, London, UK: JAI Press.

Plattner, H. and Zingsheim, H. P. (1983). Electron microscopic methods in cellular and molecular biology. *Subcell. Biochem.* **9**, 1-236.

Plattner, H., Matt, H., Kersken, H., Haacke, B. and Stürzl, R. (1984). Synchronous exocytosis in *Paramecium* cells. I. A novel approach. *Exp. Cell Res.* **151**, 6-13.

Plattner, H., Lumpert, C. J., Knoll, G., Kissmehl, R., Höhne, B., Momayezi, M. and Glas-Albrecht, R. (1991). Stimulus-secretion coupling in *Paramecium* cells. *Eur. J. Cell Biol.* **55**, 3-16.

Plattner, H., Knoll, G. and Pape, R. (1993). Synchronization of different steps of the secretory cycle in *Paramecium tetraurelia*: Trichocyst exocytosis, exocytosis-coupled endocytosis, and intracellular transport. In *Membrane Traffic in Protozoa* (ed. H. Plattner) pp. 123-148. Greenwich, CT, USA, London, UK: JAI Press.

Prescianotto-Baschong, C. and Riezman, H. (1998). Morphology of the yeast endocytic pathway. *Mol. Biol. Cell* **9**, 173-189.

Puschel, A. W., O'Connor, V. and Betz, H. (1994). The N-ethylmaleimide-sensitive fusion protein (NSF) is preferentially expressed in the nervous system. *FEBS Lett.* **347**, 55-58.

Rothman, J. E. and Wieland, F. T. (1996). Protein sorting by transport vesicles. *Science* **272**, 227-234.

Ruiz, F., Vayssié, L., Klotz, C., Sperling, L. and Madeddu, L. (1998). Homology-dependent gene silencing in *Paramecium*. *Mol. Biol. Cell* **9**, 931-943.

Ruiz, F., Beisson, J., Rossier, J. and Dupuis-Williams, P. (1999). Basal body duplication in *Paramecium* requires γ-tubulin. *Curr. Biol.* **9**, 43-46.

Sambrook, J., Fritch, E. and Maniatis, T. (1989). *Molecular Cloning: A Laboratory Manual* (2nd edn). Cold Spring Harbor, NY: Cold Spring Harbor Laboratory Press.

Söllner, T., Whiteheart, S., Brunner, M., Erdjument-Bromage, H., Geromanos, S., Tempst, P. and Rothman, J. (1993a). SNAP receptors implicated in vesicle targeting and fusion. *Nature* **362**, 318-324.

Söllner, T., Bennet, M., Whiteheart, S., Scheller, R. and Rothman, J. (1993b). A protein assembly-disassembly pathway in vitro that may correspond to sequential steps of synaptic vesicle docking, activation, and fusion. *Cell* **75**, 409-418.

Sonneborn, T. M. (1970). Methods in *Paramecium* research. *Methods Cell Physiol.* **4**, 242-335.

Sonneborn, T. M. (1974). *Paramecium aurelia*. In *Handbook of Genetics*, Vol. 2 (ed. R. C. Kung), pp. 469-594. New York: Plenum Press.

Sperling, L., Dessen, P., Zagulski, M., Pearlman, R. E., Migdalski, A., Gromadka, R., Froissard, M., Keller, A. M. and Cohen, J. (2002). Random sequencing of *Paramecium* somatic DNA. *Eukaryot. Cell* **1**, 341-352.

Tominaga, T., Allen, R. D. and Naitoh, Y. (1998a). Electrophysiology of the in situ contractile vacuole complex of *Paramecium* reveals its membrane dynamics and electrogenic site during osmoregulatory activity. *J. Exp. Biol.* **201**, 451-460.

Tominaga, T., Allen, R. D. and Naitoh, Y. (1998b). Cyclic changes in the tension of the contractile vacuole complex membrane control its exocytotic cycle. *J. Exp. Biol.* **201**, 2647-2658.

Vayssié, L., Skouri, F., Sperling, L. and Cohen, J. (2000). Molecular genetics of regulated secretion in *Paramecium*. *Biochimie* **82**, 269-288.

Vilmart-Seuwen, J., Kersken, H., Stürzl, R. and Plattner, H. (1986). ATP keeps exocytosis sites in a primed state but is not required for membrane fusion: an analysis with *Paramecium* cells in vivo and in vitro. *J. Cell Biol.* **103**, 1279-1288.

Wagner, M. L. and Tamm, L. K. (2001). Reconstituted syntaxin1A/SNAP25 interacts with negatively charged lipids as measured by lateral diffusion in planar supported bilayers. *Biophys. J.* **81**, 266-275.

Whiteheart, S. W., Schraw, T. and Matveeva, E. A. (2001). N-ethylmaleimide sensitive factor (NSF) structure and function. *Int. Rev. Cytol.* **207**, 71-112.